# MECHANICAL AND MICROSTRUCTURAL PROPERTIES OF AL 6056 FRICTION STIR WELDED JOINTS

P. Cavaliere[1], R Nobile[1], F.W. Panella[1], A. Squillace[2]
[1] Dept. of "Ingegneria dell'Innovazione", Università di Lecce, I-73100, Lecce, Italy
[2] Department of Materials and Production Engineering, University of Naples "Federico II", I-80125, Naples, Italy.

ABSTRACT

In the present paper, the effects of rotating and welding speed on the mechanical and microstructural properties of Al 6056 butt joints produced by Friction Stir Welding have been analysed. Different welding trials with variable rotating speed of the tool and different welding velocity have been done. The mechanical properties of the welded joints have been evaluated through microhardness measurements (HV) and mechanical tests at room temperature. The fatigue behaviour of the FS Welded plates under constant axial stress amplitude and load ratio $R=\sigma_{min}/\sigma_{max}=0.1$ has been investigated using a resonant testing machine for all the welded joints typologies used in the present study; the results are processed as function of the welding parameters. The microstructural evolution and grain size of the welded metal for the most interesting welding classes has been studied and correlated to micro hardness strength and the welding velocity by employing optical observations and SEM analysis.

## 1 INTRODUCTION

The Friction Stir Welding (FSW) technology is coming to be largely applied by modern aerospace industry to high performance structural applications [1]. If compared with traditional welding techniques, FSW reduces significantly the presence of distorsions and residual stresses [2-4] and ensures low cost and automation possibilities. However, the FSW process requires a complete and deep understanding of the technological process and the achieved mechanical behaviour, in order to be considered for large scale production of aeronautical components [5]. In the FSW process, a rotating tool with a specially designed probe travels down the length of the two metal plates in contact face to face; the rotating tool penetrates the contact line and produces an highly plastically deformed zone through the associated stirring action (Fig. 1). A localized thermo-mechanical affected zone is produced by friction between the tool shoulder and the plate top surfaces, as well as elevated plastic deformation of the material in contact with the tool occurs [6]. Typically, the probe depth is slightly shorter than the thickness of the work piece and its diameter is larger [7]. The FSW process is a solid state process, therefore a solidification structure is absent and the problems related to the presence of brittle inter-dendritic and eutectic phases are eliminated [8]. In addition, FSW can be used to join most of Al alloys and dissimilar materials and particular cleaning operations prior to welding are not needed, since the surface oxidation is not deterrent for the process (an alternative welding process like Resistance welding would require extensive surface preparations). In FSW the work piece does not reach the melting point and the mechanical properties of the welded zone are comparable to those provided by traditional techniques or even higher, particularly in the case of heat-treatable light alloys. In fact, the undesirable microstructure resulting from melting and re-solidification, characterized by low mechanical properties and brittleness, is avoided [9-11]. Moreover, the FS Welds are characterized by low distortions, lower residual stresses and absence of micro defects with the consequence of product retained dimensional stability.

The main parameters which characterizes the FSW process are the rotating speed of the probe and the welding speed. The present work is aimed to study the effects of these technological parameters on the mechanical and microstructural properties of 6056 FS Welded plates.

## 2 EXPERIMENTAL PROCEDURE

The material under investigation is 6056commercial aluminium alloy produced by Pechiney in the form of 4mm thickness rolled plates. Plates 200x80 mm large have been FS Welded along the rolling direction and subjected to post-weld heat treatment consisting of a former step at 170 °C for 6 h, water quenching and a latter step at 190 °C for 13 h with final water quenching; this thermal treatment has been developed by Pechiney itself and results in a considerable improvement of the corrosion resistance. The selected rotating speeds of the tool are 500, 800 and 1000 rpm, while the welding velocity is 40, 56 and 80 mm/min, obtaining totally 9 different welding classes (Tab.1). The welding nib (Fig. 1) is 6.0 mm in diameter, 3.9 mm long, and has 14 mm diameter shoulders, machined perpendicularly to the tool axis; the nib tilt angle is set equal to 3°. The Vickers hardness profiles of all the welded zones have been measured on the welded cross-section using a Vickers indenter with a 200 gf load for 15 s. The specimens for metallographic analysis have been prepared according to standard recommendations and etched with Keller's reagent to reveal the grain structure.

The mechanical tests have been performed under static and variable load in order to correlate the resulting structural properties to the welding parameters. Standard flat specimens have been cut along the direction perpendicular to the weld line with an electrical discharge machine (EDM). The tensile tests have been performed at room temperature using an MTS 810 testing machine with cross-head speed of $10^{-3}$ mm/s. HCF fatigue tests have been executed with a RUMUL Testronic 50±25 kN resonant testing machine. They have been conducted with constant stress amplitude under axial load with $R = \sigma_{min}/\sigma_{max} = 0.1$ until complete failure occurs. The frequency, depending on the specimen and fittings stiffness, varies from 150 to 200 Hz.

## 3 RESULTS AND DISCUSSION

FSW is becoming a very efficient method to overcome the Al sheet joining problems for aerospace industry, since good ductility and high strength can be achieved, in conjunction with elevated process velocity and automation characteristics. In the present work, FSW butt welds of AA6056 sheets have been successfully achieved with different process parameters. Table 1 resumes the welding parameters of the nine welded joints classes, while Table 2 reports the base material tensile properties.

In Figure 2 a-c, the stress-strain curve for the tensile behaviour of the welded specimens at room temperature for all the welding classes are showed. All the welded joints except All-3 type assure elevated ultimate resistance values ($\sigma_u$ in the range of 230-280 MPa) and elongation capabilities; the optimal tool rotation velocity is found to be over 800 rpm, while the welding velocity seems not to have significant influence on static strength. A strong ductility variation, qualitatively estimated as true strain to fracture, is described in Fig. 3 and the yield strength is analysed as a function of the welding parameters in Fig. 4. The material ductility reaches the higher values with welding velocity around 40 and 56 mm/min and when the tool rotating speed is low (500 rpm); when the rotating speed and the welding velocity increase, a remarkable and general ductility drop is noticed. At the contrary, the higher tensile strength is reached in correspondence with higher rotating speeds (800 and 1000 rpm) and higher welding velocity used in the present experiments (80 mm/min). The extreme variability of the FS Welded joints ductility is also accompanied by relevant grain size variation and distribution observed after optical microscopy. As good compromise, a beneficial welding parameters choice is claimed to set the welding velocity and tool speed equal respectively to 56 mm/min and 800 rpm.

The fatigue Wöhler curves of the FSW joined specimens are presented in Figures 5-7. A number of 5 specimens for each of the 9 welded classes has been tested; despite this number is insufficient for definitive fatigue analysis, some considerations can be arisen for the present work.

The fatigue curves have been extrapolated from data up to $10E^6$ cycles; at welding velocity of

40mm/min (Fig. 5) the welded joints have similar behaviour with steep slope and moderate scatter in both the low and high cycle ranges for all the tool speeds; in addition, all the specimens reveal good fatigue properties when the cycle number is in the range of 50.000-200.000. Longer life can be reached only with significant stress amplitudes decrease; the fatigue stress limit is presumably positioned below 55 MPa.
In Figures 6 and 7, the fatigue curves referred to welding velocity equal to 56 and 80mm/min respectively with different tool speeds are described; it can be remarked a similar trend to the previous Wöhler curves, since the fatigue resistance is still elevated at low cycle ranges and generally drops down immediately after 200.000 cycles; welded classes All-2 and All-9 seem to behave better at higher cycle number, around $10E^6$, while all other welding classes keep poor fatigue strength in correspondence to longer life.
More over, the specimens joined with high welding speed in the range of 800-1000 rpm show the best fatigue behaviour in the low cycle range, reaching $\sigma_a$=90 MPa; the response of the welded material modifies in the high cycle range, in which the specimens welded with 500 rpm tool speeds seems to exhibit higher cycles to failure at the same stress level.
In the range of the selected welding and rotating speeds, the specimens welded with higher welding velocity, 56 and 80 mm/min, show a better behaviour in the high cycle regime for any tool speed, since $\sigma_a$ is settled around 60 MPa at $10E^6$ cycles. A better comprehension of the fatigue data is done in Figure 8, where the stress amplitude corresponding to an averaged reference life of $10^5$ number of cycles to failure as function of the welding conditions is shown. The specimens joined with a welding velocity of 56 mm/min clearly produce better fatigue endurance for any tool speeds, according to satisfying ductility and yield strength requirements; a more stable fatigue behaviour and increased ductility can be reached adjusting the tool rotating speed.
The microhardness profiles of the FSW joints have been measured in the welded cross sections for all the FS Welded classes. An example of microhardness plot (Hv1) vs. distance from the weld axis is shown in Fig. 9 for the welding velocity of 80 mm/min. The profiles appear continuous and uniform for all the welded plates with average value of 110 Hv, particularly for the lower rotating speed (500 rpm) and the lower welding velocities ( 40 and 56 mm/min). Using higher rotating and welding speeds, the material hardness reaches higher values around 160 Hv and the profiles become steeper and extremely variable across the weld centre.
The microstructural behaviour of 6056 aluminium alloy is described in Figures 10-11, where the micrographs of the nugget zones centre of samples All-5 and All-6 respectively. The material microstructure appears with very fine and equiaxed grains and without voids and other significant defects in all the welding conditions. Subsequently, the grains mean area has been measured with an image analyser on a number of 100 grains for each condition; the grain size variation is plot vs. the FS Welding parameters is shown in Fig. 12. An interesting dependence on the welding speed can be noticed, while the tool speed seems not to have any influences.
; it can be concluded that the grain size evolution of the material in the nugget zone has a strong influence on the fatigue behaviour of the studied Friction Stir Welded aluminium alloy sheets.
The maximum microhardness has been also correlated to the average grain size in the same measure point (Fig. 13); a clear relation of the mean grain size of the differently welded specimens with the mechanical capabilities, indicated by the microhardness, is remarked. In fact, the microstructural evolution is a direct consequence of the welding parameters and strongly influences the mechanical microhardness and strength.
FEGSEM observations have been finally performed on the fractured surfaces of the tensile tested specimens for the different welding conditions. In Figure 14 a-b, the rupture surfaces of specimens welded with 800 RPM tool speed and welding velocities 56 and 80 mm/min are respectively presented. The images showed an uniform distribution of very fine dimples with different dimensions, according to the different welding conditions; the dimples structure is due

either to the fine initial grain sizes of the base material, either to the welding process. The mean dimples dimensions has been observed to decrease as incrementing the welding velocity.

## 4 CONCLUSIONS

The microstructural and mechanical behaviours of 6056 Friction Stir Welded aluminium alloy sheets using three different welding velocities (40, 56 and 80mm/min) and three different tool rotation speeds (1000, 800 and 500 rpm) have been studied. The tensile tests performed at room temperature showed the material ductility to reach the higher values with 40 and 56 mm/min welding velocities and lower rotating speed (500 rpm). On the other hand, high tensile strength is assured in correspondence of higher rotating speeds (800 and 1000 rpm) and higher welding velocity (80 mm/min). The fatigue endurance data showed similar material response as a function of the different processing parameters, though the better configuration is achieved with welding speed equal to 56 mm/min. The microhardness profiles (Hv) appear uniform for the plates joined using the lower rotating speed (500 rpm) and the lower welding velocity (40 and 56 mm/min). Applying higher rotating and welding speeds, the hardness reaches higher values for all the welding conditions and the profiles become more fluctuating across the weld centre. The microstructure of the welded metal reveals very fine and equiaxed grains for all the welding conditions and coherent dimples distribution is detected on ruptured surfaces.

## REFERENCES


1. W. M. Thomas, E. D. Nicholas, J . C. Needam, M. G. Murch, P . Templesmith and C. J . Dawes, GB Patent Application No. 9125978.8, December 1991 and US Patent No. 5460317, October 1995.
2. G. Bussu, P.E. Irving, “The role of residual stress and heat affected zone properties on fatigue crack propagation in friction stir welded 2024-T351 aluminium joints”, International Journal of Fatigue 25 (2003) 77–88.
3. R.John, K.V. Jata and K. Sadananda, “Residual stress effects on near threshold fatigue crack growth in friction stir welded aerospace alloys,“ International Journal of Fatigue, 25, (2003) 939-948.
4. K.V. Jata, K.K. Sankaran and J. Ruschau, “Friction-stir welding effects on microstructure and fatigue of aluminum alloy 7050-T7451,” Metallurgical and Materials Transactions, September 2000: 31A, 2181-2192.
5. W. D. Lockwood, B. Tomaz, A.P. Reynolds, “Mechanical response of friction stir welded AA2024: experiment and modelling”, Materials Science and Engineering A323 (2002) 348–353.
6. M. Guerra, C. Schmidt, J.C. McClure, L.E. Murr, A.C. Nunes, “Flow patterns during friction stir welding”, Materials Characterization 49 (2003) 95– 101.
7. P. Ulysse, “Three-dimensional modeling of the friction stir-welding process”, International Journal of Machine Tools & Manufacture 42 (2002) 1549–1557.
8. C.G. Rhodes, M.W. Mahoney, W.H. Bingel, “Effects of Friction Stir Welding on microstructure of 7075 aluminium”, Scripta Materialia 36 (1997) 69–75.
9. Yutaka S. Sato, Mitsunori Urata, Hiroyuki Kokawa, Keisuke Ikeda, “Hall- Petch relationship in friction stir welds of equal channel angular-pressed aluminium alloys”, Materials Science and Engineering A354 (2003) 298-305.
10. Patrick B. Berbon, William H. Bingel, Rajiv S. Mishra, Clifford C. Bampton, Murray W. Mahoney, “Friction Stir Processing: A Tool To homogenize Nanocomposites Aluminum Alloys”, Scripta mater. 44 (2001) 61–66.
11. W.B. Lee, Y.M. Yeon, S.B. Jung, “The improvement of mechanical properties of friction-stir-welded A356 Al alloy”, Materials Science and Engineering A355 (2003) 154-159.

| Welding class | All 1 | All 2 | All 3 | All 4 | All 5 | All 6 | All 7 | All 8 | All 9 |
|---|---|---|---|---|---|---|---|---|---|
| Tool rotating speed [rpm] | 500 | 500 | 500 | 800 | 800 | 800 | 1000 | 1000 | 1000 |
| Welding Velocity [mm/min] | 40 | 56 | 80 | 40 | 56 | 80 | 40 | 56 | 80 |

Table 1: Welding classes according to tool rotating and welding speeds.

| Alloy | $\sigma_y$ (MPa) | $\sigma_u$ (MPa) | Elongation (%) | $\sigma_a$ at $10E^6$ cycles (MPa) |
|---|---|---|---|---|
| 6056 T4 | 240 | 316 | 23 | 98 |

Table 2: Tensile properties of the 6056 Al alloy.

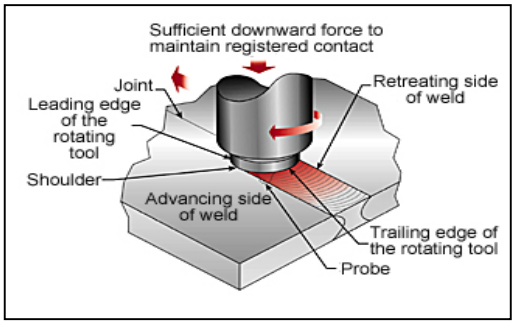


Fig. 1: The FSW Process and the tool geometry.

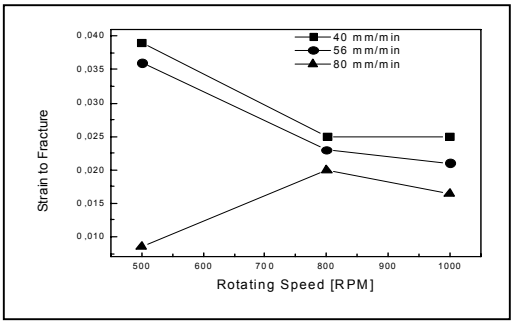


Fig. 3: Ductility Behaviour of the welded plates.

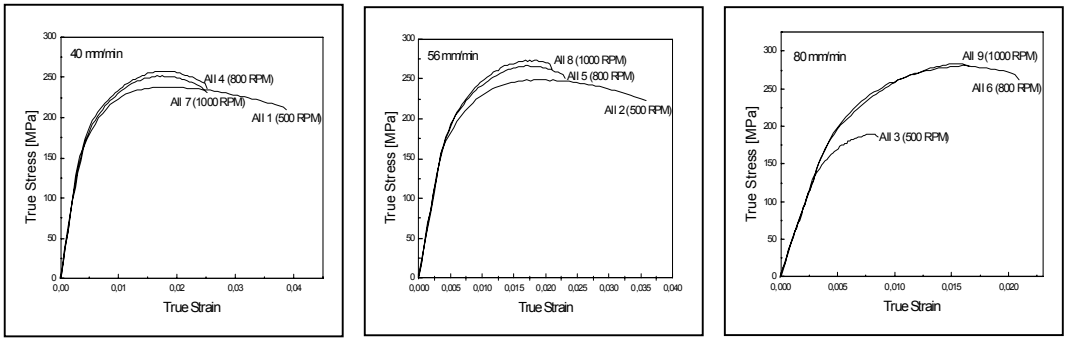


Fig. 2: Stress-Strain curves for all the 6056 aluminium alloy welded classes.

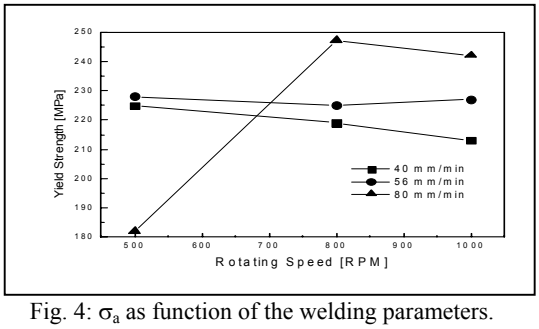


Fig. 4: $\sigma_a$ as function of the welding parameters.

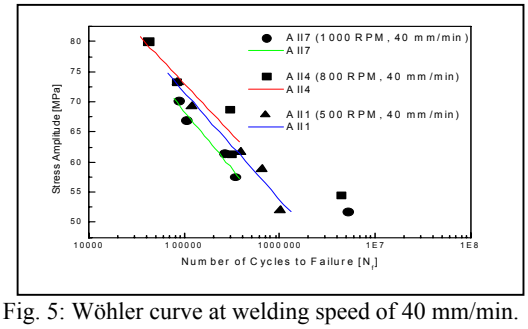


Fig. 5: Wöhler curve at welding speed of 40 mm/min.

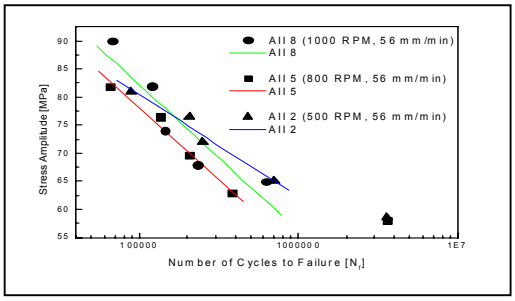


Fig. 6: Wöhler curve at welding speed of 56 mm/min.

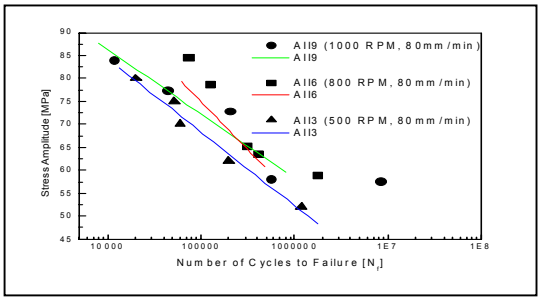


Fig. 7: Wöhler curve at welding speed of 80 mm/min.

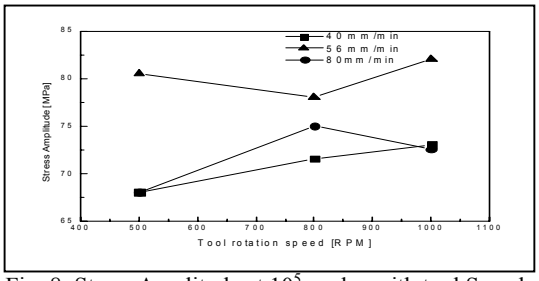


Fig. 8: Stress Amplitude at $10^5$ cycles with tool Speed.

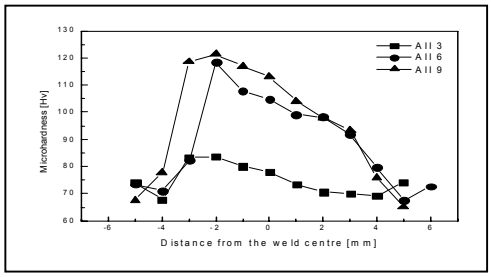


Fig. 9: Microhardness profile example.

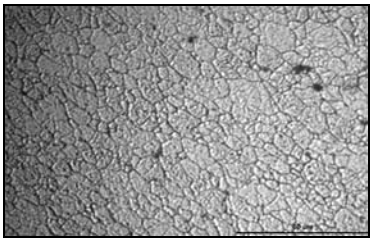

Fig. 10: Grain size and distribution for All-5 welds.

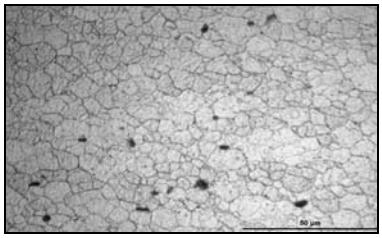

Fig. 11: Grain size and distribution for All-6 welds.

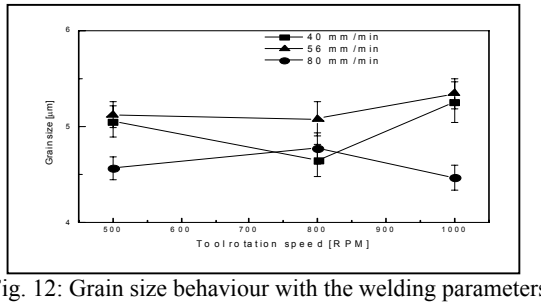


Fig. 12: Grain size behaviour with the welding parameters.

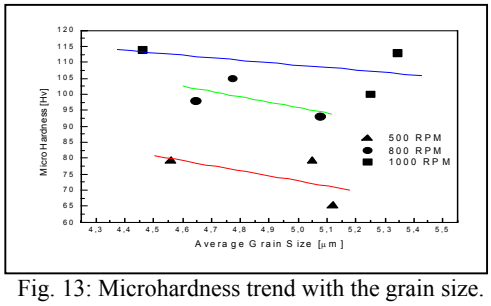


Fig. 13: Microhardness trend with the grain size.

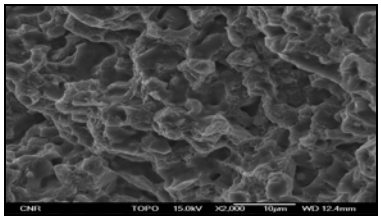

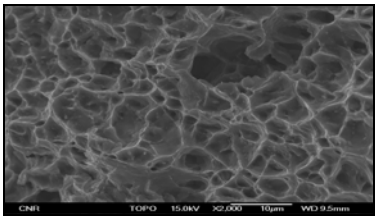

Fig. 14 a-b: SEM microstructure for optimal welds.